Localization effects on the vibron shifts in helium-hydrogen mixtures

Sam B. Ramsey, Miriam Pena-Alvarez, and Graeme J. Ackland
Centre for Extreme Conditions, School of Physics and Astronomy, The University of Edinburgh, Edinburgh EH9 3FD, Scotland, United Kingdom

(Received 28 July 2019; revised manuscript received 16 October 2019; accepted 16 April 2020; published 4 June 2020)

The vibrational frequency of hydrogen molecules has been observed to increase strongly with He concentration in helium-hydrogen fluid mixtures. This has been associated with He-H interactions, either directly through chemical bonding [Lim and Yoo, Phys. Rev. Lett. **120**, 165301 (2018)] or indirectly through increased local pressure [Loubeyre *et al.*, Phys. Rev. B **32**, 07611 (1985)]. Here, we demonstrate that the increase in the Raman frequency of the hydrogen molecule vibron is due to the number of H_2 molecules participating in the mode. There is no chemical bonding between He and H_2; helium acts only to separate the molecules. The variety of possible environments for H_2 gives rise to many Raman-active modes, which causes broadening of the vibron band. As the Raman-active modes tend to be the lower-frequency vibrons, these effects work together to produce the majority of the shift seen in experiment. We used density functional theory (DFT) methods in both solid and fluid phases to demonstrate this effect. DFT also reveals that the pressure in these H_2-He mixtures is primarily due to quantum nuclear effects; again, the weak chemical bonding makes it a secondary effect.

DOI: 10.1103/PhysRevB.101.214306

I. INTRODUCTION

Hydrogen and helium are the simplest and most abundant elements in the universe. As such, the recent claim that there is chemical bonding between hydrogen and helium is potentially transformative to understanding their high-pressure interactions for both the condensed-matter and astrophysical communities [1]. The lightness of each element means that nuclear motion and zero-point effects play a large part in their dynamics, so that standard methods of electronic structure calculation are insufficient to describe them. This gives rise to exotic phases of matter such as superfluids and, potentially, supersolids [2,3]. The understanding of mixtures of hydrogen and helium under pressure is important for the study of the gas giants such as Jupiter and Saturn as they are the primary constituents [4–6]. It is also important to characterize the mixtures as helium is commonly used as a pressure medium in diamond anvil cell (DAC) experiments [7].

Helium and molecular hydrogen are readily miscible in the fluid regime. DAC experiments of <10 GPa see a single fluid phase with the characteristic signal being the Raman-active mode of the hydrogen vibron [8]. The vibron frequency is seen to be blueshifted in mixtures, with the magnitude of this shift being dependent on the relative concentration of the mixture. This has been variously attributed to an effective increase of pressure induced on the hydrogen molecule due to the helium solution [8,9], although no amount of pressure can cause such a large shift in pure hydrogen, and to novel chemical bonding [1]. At higher pressures, first H_2 and then He solidify into hexagonal close-packed solids and demix, perhaps causing "He rain" (or, more properly, snow) in planetary atmospheres. Weak H_2 vibrons have been observed in the He-rich solid [1], suggesting low solid solubility.

Helium and hydrogen have been known to form stable alloys with other noble gases [10–13]. A similar frequency shift is seen in the Raman spectrum of the hydrogen compounds. This suggests that the effect is caused by coupling between hydrogen molecules weakening as they are separated by the chemically inert elements [14–16]. A simple classical molecular potential with nearest-neighbor interactions has shown that this effect is of the right order of magnitude to explain the behavior in argon-hydrogen mixtures [14,17]. Here we present a first-principles investigation of this effect in helium-hydrogen mixtures to accurately describe the observed experimental effects.

II. METHODS

To study the system, density functional theory calculations were carried out on mixtures of helium and hydrogen at various concentrations. Previous work has concentrated on astrophysically relevant conditions, <100 GPa and <1000 K, where van der Waals interactions and nuclear quantum effects can be safely ignored [6,18,19]. Our calculations are at relatively low pressures and require van der Waals interactions, which are accounted for using a Grimme dispersion scheme and a Perdew-Burke-Ernzerhof functional [20–22]. Moreover, below 5 GPa, the largest contribution to the pressure comes from quantum nuclear effects: the pressure arising from changes in zero-point energy (ZPE) with density. To account for this, we carry out standard Nose-Parrinello-Rahman (NPT) calculations, as implemented in CASTEP [23], then use lattice dynamics and the quasiharmonic approximation to calculate the true pressure. There is no analytic form for the variation of the zero-point energy with volume within DFT. So, in practice, this requires calculation of the free energy as a function of volume and temperature $G(V, T)$, for cells relaxed

in the NPT ensemble to have isotropic stress and including the zero-point energy. We then perform a numerical Legendre transform on the grid of $G(V, T)$ to obtain $G(P, T)$.

We used a molecular dynamics calculation to model the fluid state, and used a geometry optimized hexagonal close-packed (hcp) lattice for the solid. Hydrogen molecules and He atoms were randomly distributed to produce various concentrations, with all molecular dynamics calculations being carried out at 300 K.

Several-thousand molecules are required to fully describe the liquid structure [24], but the phonon density of states is well sampled in much smaller cells. Density functional perturbation theory (DFPT) was used to calculate Raman activity and the vibrational contribution to the pressure. Simulation cells of 36 molecules were used for both fluid and solid regimes. To capture the disordered structure of the fluid regime, molecular dynamics calculations were carried out for 1 ps at 300 K before snapshots were taken. Five snapshots were taken from each molecular dynamics run to ensure proper sampling of atomic configurations. The resulting snapshots were then relaxed to a local minimum so that DFPT calculations could be carried out (see Supplemental Material [25]). This allowed us to simulate the hydrogen vibron, which occurs over relatively short timescales, including the effects of the disordered fluid without the computational cost of large molecular dynamics simulations. The enthalpy was converged to 1 meV using a $2 \times 2 \times 2$ k-point grid. Van der Waals functionals are essential for helium; however, it is also well known that these functionals overestimate the hydrogen vibron frequency [26]. To facilitate comparison with the experimental results, calculated frequencies are shifted by 126 cm^{-1} to match the experimental hydrogen vibron. The high-pressure calculations shown in the inset of Fig. 2 were carried out using simulation cells of 96 molecules and a $3 \times 3 \times 3$ k-point grid. All calculations are carried out using the CASTEP code [23].

III. RESULTS AND DISCUSSION

While solid helium at these pressures has been well studied using classical potentials, here we use a fully quantum treatment of the electrons. *Ab initio* methods have the advantage of reliably working with multiple elements over a wide range of pressures [27,28]. Figure 1 demonstrates that while van der Waals effects are important, the dominant contribution to the pressure comes from quantum nuclear effects, and that these have a massive effect on the equation of state, shifting the equilibrium density in pure He by about 50%.

The effect of increasing He concentration in these calculations is to blueshift the vibron and to reduce the ZPE pressure. In Fig. 2, the calculated frequencies at different He concentrations at different pressures are presented together with experimental results [1,29]. The frequencies' changes are in good agreement with the experimental results. Analysis of the vibron eigenmodes shows negligible participation of the He atoms in the motion, demonstrating the absence of chemical interactions between helium and hydrogen. This suggests that the observed *blueshift* with increasing helium concentration is due to fewer couplings between adjacent H_2 molecules and localization of the vibrational modes.

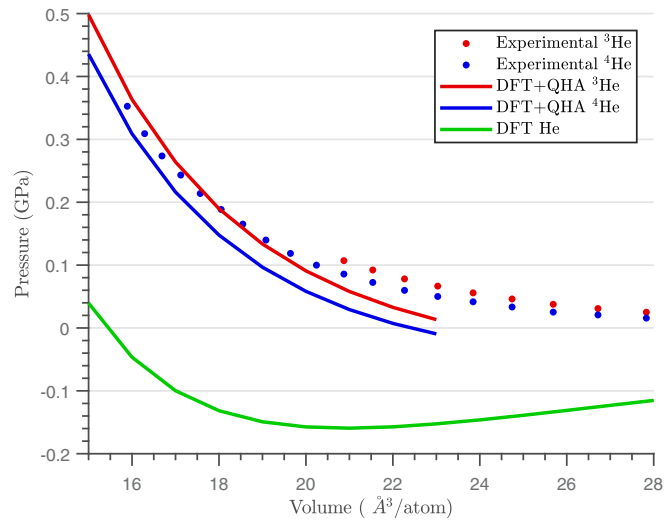

FIG. 1. Equation of state of both helium isotopes in the hcp structure. The DFT calculations use Grimme–van der Waals corrections, for which hcp is stable against bcc and fcc. The green (lower) line shows the equation of state in the Born-Oppenheimer approximation. Blue (middle) and red (upper) curves show the effect of adding zero-point pressures in the quasiharmonic approximation. Above 20 Å^3/atom, the static relaxations give negative pressure, and above 23 Å^3/atom, the hcp structure cannot be stabilized without ZPE. Experimental data are from x-ray and strain gauge measurements [30–33].

To determine miscibility within the solid regime, we examined H_2 impurities in helium. Both hydrogen and helium atoms form HCP solid phases in this pressure regime, and the enthalpy of solution, means hydrogen can only occupy substitutional sites in the solid helium lattice (Table I). At room temperature, the calculated solubility limit is 0.2%. This is in keeping with the existing literature [5,6,34,35]. Measuring such a small concentration experimentally is challenging: a weak vibron signal in the He-rich fluid has been noted [1], but another recent paper shows no signal [36] despite indicating solubility up to 10% (Fig. S1 in that paper).

Table II shows the binding energy for clusters of substitutional hydrogen molecules compared with isolated hydrogen molecules in solid helium. All the enthalpies of formation are negative and become larger as more hydrogen is added, a strong suggestion that when within a helium lattice, hydrogen molecules tend to cluster as they attract one another. Standard DFT calculations suggest strong H_2-H_2 interactions, relative to He-He, but unexpectedly this difference is significantly reduced when the ZPE is accounted for through DFPT. Nevertheless, below room temperature, the binding is close to the configurational entropy cost, so significant numbers of H_2 microclusters can be expected. The vibrons associated with H_2 solutes are significantly blueshifted from the pure H_2 value due to the lack of coupling, with the single substitutional having the largest shift, perhaps accounting for the multiple Raman peaks attributed to interstitials by Yoo *et al.* [1].

Recent experimental results have claimed that at room temperature and pressures above 12 GPa, helium and hydrogen are able to chemically bond [1,37]. The experimental evidence for chemical association comes from another

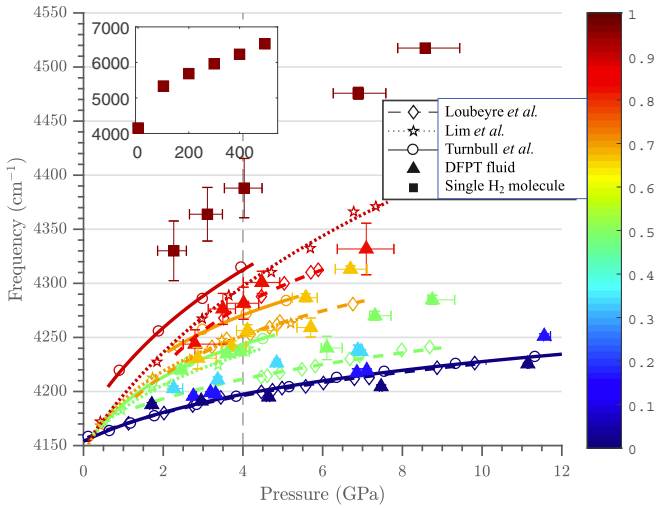

FIG. 2. Comparison of experimental and calculated pressure-frequency relation with color coding used to show the atomic fraction of helium (X_{He}). The color scale represents the concentration of helium: only data of the same color should be compared. The lowest helium concentrations shown are pure hydrogen and the highest have a single hydrogen molecule in the simulation cell. Experimental data taken from Turnbull *et al.* [29], Lim *et al.* [1], and Loubeyre *et al.* [8] are plotted against DFT results from the fluid regime for a range of concentrations and pressures. All experimental data are fitted with a logarithmic function. A more direct comparison of concentration and frequency is given in Fig. 3. The Raman and phonon density of states shown in Fig. 3 are taken at 4 GPa as denoted by the gray vertical line. The inset shows the frequency of the isolated hydrogen molecule vibron up to 500 GPa. All frequencies have been shifted by 126 cm^{-1} to account for the functionals overbinding of hydrogen molecules [26]. Pressures and horizontal error bars are found by fitting each concentration to a Birch-Murnaghan equation of state. Vertical error bars are simply the standard deviation of the five samples taken from each molecular dynamics calculation.

vibrational mode observed at around 2400 cm^{-1}. We do not see any evidence of any vibrational modes in this frequency range in our calculations. Other studies [29,35] have demonstrated that this effect could be due to nitrogen contamination. If, as we propose, the concentration dependence is due simply to the number of hydrogens participating in the modes, then the effect will be largely independent of whether the hydrogen is diluted by He or N_2: by contrast, He-H_2 chemical bonding or local stresses [9] will depend on the composition of the solvent. The experiments show consistent vibron shifts with H_2 concentration, regardless of nitrogen content [1,29].

TABLE I. The enthalpy and energy cost of including hydrogen atoms in hcp helium at 12 GPa for each site is given. The miscibility ($e^{-\Delta H/kT}$) at 300 K is calculated assuming a dilute regular solid solution.

	ΔH (eV)	ΔE (eV)	Miscibility
Substitutional	0.164	0.048	0.2%
Tetrahedral	0.552	1.267	2×10^{-7}%
Octahedral	0.640	1.032	5×10^{-6}%

TABLE II. Formation energy for clusters of substitutional hydrogen molecules compared with a lone hydrogen molecule in an hcp helium lattice. Results with and without accounting for zero-point energy are shown, along with the configurational entropy cost to the free energy at room temperature.

	ΔE	ΔE+ZPE (eV)	$k_B T \ln N$
Pair	−0.043	−0.006	0.017
Triplet	−0.114	−0.023	0.025
Quadruplet	−0.185	−0.037	0.034

As shown in Fig. 2, an isolated hydrogen molecule (represented by the $X_{He} = 0.9722$) in a helium mixture has a significantly higher Raman frequency than pure hydrogen at the same pressure. Figure 3 shows that as X_{He} concentration decreases, the phonon density-of-states band is both *broadened* and *shifted*. The apparent phonon-frequency shift due to concentration is enhanced by the broadening (Fig. 5) because Raman activity tends to be stronger for the lower-frequency vibron modes. DFPT calculations in the fluid reveal that even the Raman peak arises from several modes. The in-phase vibration of all molecules in a cluster is the strongest, but in the absence of symmetry many other modes acquire some Raman activity. These modes have slightly higher frequency than the in-phase vibron, and so cause a skew in the peak shape in Fig. 4.

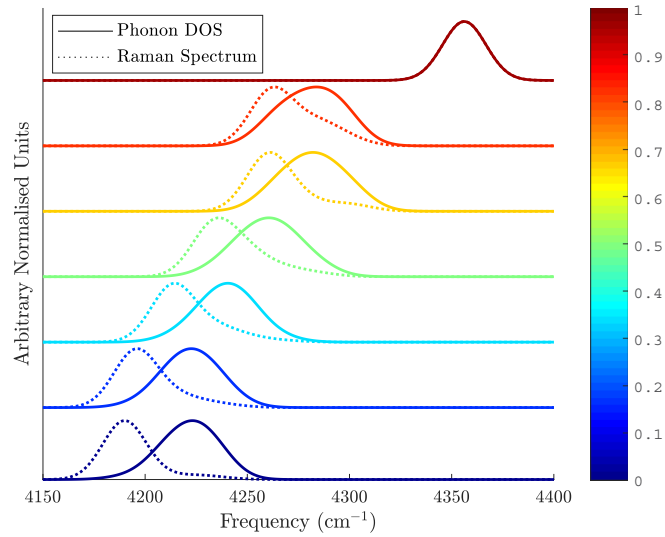

FIG. 3. Phonon density of states and associated Raman intensities for a range of concentrations is taken from DFPT calculations carried out in the fluid model showing how the hydrogen vibron mode changes with concentration (color bar shows He concentration). The phonon density of states broadens and the average frequency blueshifts shifts as the He concentration is increased. As the strongest Raman-active mode is the lowest frequency of the phonon band, this results in the Raman intensities diverging from the phonon density of states at lower He concentration. Weaker Raman modes give a pronounced high-frequency "tail" to the Raman peak. All peaks fitted with a 25 cm^{-1} FWHM Gaussian broadening. These spectra have been taken at 4 GPa as indicated by the gray doted line in Fig. 2.

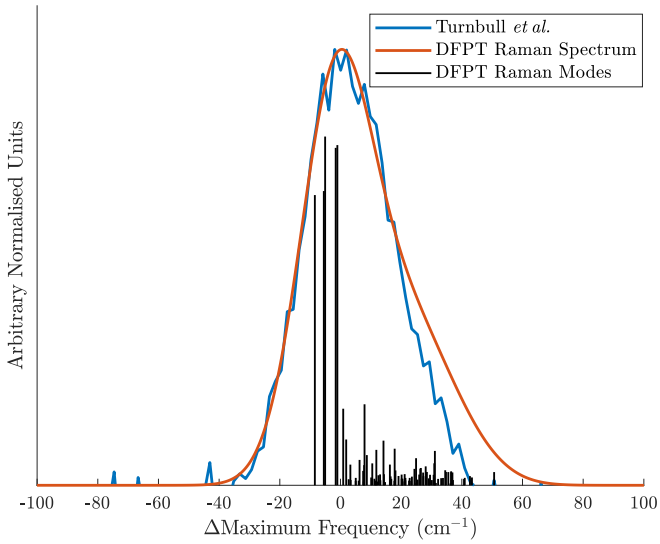

FIG. 4. Comparison of experimental Raman peak with DFT data at 2.7 GPa and 50% H_2 concentration. The DFPT Raman intensities shown in black are convolved with a 28 cm^{-1} Gaussian broadening to get the resulting spectrum. Blue experimental data were collected during a previous campaign [29]. Both the experimental and DFT spectra are asymmetric with a high-frequency tail. This effect is due to the weaker, but still active Raman modes at higher frequency. Raman modes from all five snapshots taken at this pressure are shown in the figure.

A comparison of the panels in Fig. 5 provides strong evidence that the frequency shift is due to localization, which we measure as the inverse participation ratio:

$$\frac{\sum_i \mathbf{e}_i^4}{\left(\sum_i \mathbf{e}_i^2\right)^2},$$

where $\mathbf{e}_i$ is the mode displacement vector of each atom i. The larger the number of hydrogen atoms participating in a vibron mode, the lower its frequency. An isolated hydrogen molecule has the highest frequency, while the lowest observed mode occurs in pure solid hydrogen, where the Raman mode involves all molecules vibrating together. The shift and multiplicity of the peaks due to species and fluid disorder are similar to the isotope disorder effect in hydrogen [38,39].

These effects are seen in both the solid and the fluid. However, the solid vibron shift is larger because the pure H_2 fluid vibron is already partially localized due to the disordered nature of the fluid. At high H_2 concentrations, the differences between solid and fluid are largest: all hydrogens have many coupled neighbours, but the fluid vibron is still localized due to the disorder.

The comparison with the experimental fluid measurements shows that the main effects that are involved in the frequency shift are qualitatively reproduced in this model. The primary experimental evidence of solid phase miscibility is the observation of an H_2 vibron mode in the helium [1]. Consistent with our calculations for *substitutional* and *clustered* H_2, these observed modes are blueshifted with the less-blueshifted cluster mode being broader. It was not possible to determine a precise H_2 concentration in the experiment [40], but our calculated solubility is sufficient to produce an observable

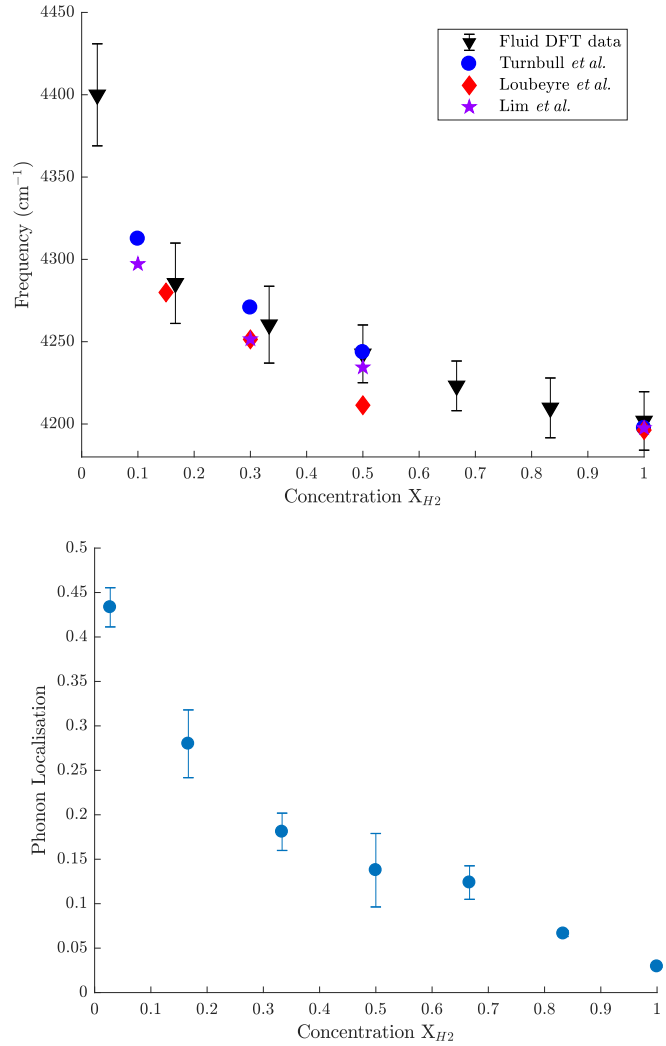

FIG. 5. (a) DFPT calculation plotted against experimental results [1,8,29], showing the change in Raman-active vibron due to the change in mixture composition at 4 GPa. DFPT frequencies at precisely 4 GPa are interpolated from the data shown in Fig. 2. Error bars on the DFPT data are taken from the root-mean-square error of the fits to the data in Fig. 2. (b) Calculations of the inverse participation ratio of the calculated strongest Raman-active phonon modes. The error bars are taken from the standard deviation of three independent configurations in the solid regime at each concentration.

signal and therefore the calculations support the experimental data [1].

In our DFPT calculations, we have assumed that two elements are randomly distributed throughout the mixtures. However, if the hydrogen molecules are more clustered, this would enhance coupling and drive down the vibron frequency of the high X_{He} mixtures. To understand the potential magnitude of this effect, DFPT calculations were carried out on a simulation cell with $X_{He} = 0.8333$ with a single cluster of hydrogen molecules: This resulted in a drop in frequency of 22 cm^{-1} and reduced inverse participation ratio. Thus we show that localization increases the frequency, independent of concentration.

Our results may serve as a reference for future works on mixtures and alloys in general, and on hydrides in particular.

Experimental mixtures are sometimes prepared *in situ* and the real concentration of the components may not be known. However, here we show a relationship between Raman shift, pressure, and hydrogen concentration which could be used as a reference for concentration calibrations. On the other hand, this work highlights that attention should be paid not only to the shifting of the vibrons, but also to the width as it can provide important information about concentrations and intermolecular interactions. Here we characterize a system in which a hydrogen molecule can be confined without chemical interaction. These isolated hydrogen molecules act as an analogy for a confined hydrogen molecule, which may in the future be compared directly to experiment. As shown in the inset of Fig. 2, the frequency of the isolated hydrogen molecule in the helium pressure medium continues to increase as the pure hydrogen's frequency decreases. This demonstrates the importance of coupling effects even at higher pressures.

IV. CONCLUSIONS

In conclusion, we have carried out an *ab initio* study of the hydrogen molecular vibron in HeH_2 mixtures. We show that including van der Waals corrections and zero-point-energy effects is essential to reproducing the equation of state below 10 GPa. The vibron blueshift with increasing He concentration is shown to be due to the reduction of hydrogen-hydrogen coupling and the associated localization of the vibrational mode. "Local pressure" effects can be ruled out because the isolated hydrogen molecule in He has a significantly higher vibron frequency than pure hydrogen at any pressure. The observed broadening of the vibron in mixtures is because there are Raman-active vibrations involving various numbers of H_2 atoms. The calculations support the possibility of small amounts of H_2 existing as substitutional impurities in solid He, but unequivocally rule out interstitial H_2 or any He-H_2 chemical bond.

Note added. Recently, some results in this paper regarding solid phases at 0 K have been replicated elsewhere [35].

ACKNOWLEDGMENTS

We acknowledge E. Gregoryanz and R. Howie for useful discussions and for sharing their primary data, and C. S. Yoo regarding the observability of low-H_2 concentrations in the He-rich fluid. G.J.A. and M.P.A. were supported by the ERC Hecate project, and S.B.R. acknowledges a studentship from EPSRC. Computing resources were provided by UKCP (EPSRC Grant No. EP/P002790).

[1] J. Lim and C.-S. Yoo, Phys. Rev. Lett. **120**, 165301 (2018).
[2] N. Prokof'ev and B. Svistunov, Phys. Rev. Lett. **94**, 155302 (2005).
[3] E. Kim and M. Chan, Nature (London) **427**, 225 (2004).
[4] T. Guillot, Planet. Space Sci. **47**, 1183 (1999).
[5] J. M. McMahon, M. A. Morales, C. Pierleoni, and D. M. Ceperley, Rev. Mod. Phys. **84**, 1607 (2012).
[6] M. A. Morales, E. Schwegler, D. Ceperley, C. Pierleoni, S. Hamel, and K. Caspersen, Proc. Natl. Acad. Sci. **106**, 1324 (2009).
[7] A. Jayaraman, Rev. Mod. Phys. **55**, 65 (1983).
[8] P. Loubeyre, R. Le Toullec, and J. P. Pinceaux, Phys. Rev. B **36**, 3723 (1987).
[9] P. Loubeyre, R. Le Toullec, and J.-P. Pinceaux, Phys. Rev. B **32**, 7611 (1985).
[10] C. Cazorla and D. Errandonea, Phys. Rev. B **81**, 104108 (2010).
[11] C. Cazorla, D. Errandonea, and E. Sola, Phys. Rev. B **80**, 064105 (2009).
[12] A. K. Kleppe, M. Amboage, and A. P. Jephcoat, Sci. Rep. **4**, 4989 (2014).
[13] C. Ji, A. F. Goncharov, V. Shukla, N. K. Jena, D. Popov, B. Li, J. Wang, Y. Meng, V. B. Prakapenka, J. S. Smith *et al.*, Proc. Natl. Acad. Sci. **114**, 3596 (2017).
[14] P. Loubeyre, R. LeToullec, and J. P. Pinceaux, Phys. Rev. B **45**, 12844 (1992).
[15] M. I. M. Scheerboom and J. A. Schouten, Phys. Rev. B **53**, R14705 (1996).
[16] E. W. Knapp and S. F. Fischer, J. Chem. Phys. **76**, 4730 (1982).
[17] B. Silvi, V. Chandrasekharan, M. Chergui, and R. D. Etters, Phys. Rev. B **33**, 2749 (1986).
[18] J. M. McMahon and D. M. Ceperley, Phys. Rev. B **85**, 219902(E) (2012).
[19] N. Nettelmann, B. Holst, A. Kietzmann, M. French, R. Redmer, and D. Blaschke, Astrophys. J. **683**, 1217 (2008).
[20] J. P. Perdew, K. Burke, and M. Ernzerhof, Phys. Rev. Lett. **77**, 3865 (1996).
[21] S. Grimme, J. Comput. Chem. **27**, 1787 (2006).
[22] J. Klimeš and A. Michaelides, J. Chem. Phys. **137**, 120901 (2012).
[23] M. D. Segall, P. J. D. Lindan, M. J. Probert, C. J. Pickard, P. J. Hasnip, S. J. Clark, and M. C. Payne, J. Phys.: Condens. Matter **14**, 2717 (2002).
[24] H. Y. Geng, Q. Wu, M. Marques, and G. J. Ackland, Phys. Rev. B **100**, 134109 (2019).
[25] See Supplemental Material at http://link.aps.org/supplemental/10.1103/PhysRevB.101.214306 for representative atomic positions from fluid calculations, and input files for CASTEP calculations.
[26] S. Azadi and G. J. Ackland, Phys. Chem. Chem. Phys. **19**, 21829 (2017).
[27] Y. A. Freiman, S. M. Tretyak, A. Grechnev, A. F. Goncharov, J. S. Tse, D. Errandonea, H.-K. Mao, and R. J. Hemley, Phys. Rev. B **80**, 094112 (2009).
[28] C. Cazorla and J. Boronat, Phys. Rev. B **91**, 024103 (2015).
[29] R. Turnbull, M.-E. Donnelly, M. Wang, M. Peña Alvarez, C. Ji, P. Dalladay-Simpson, H.-K. Mao, E. Gregoryanz, and R. T. Howie, Phys. Rev. Lett. **121**, 195702 (2018).
[30] H.-K. Mao, R. J. Hemley, Y. Wu, A. P. Jephcoat, L. W. Finger, C. S. Zha, and W. A. Bassett, Phys. Rev. Lett. **60**, 2649 (1988).
[31] G. Straty and E. Adams, Phys. Rev. **169**, 232 (1968).
[32] R. L. Mills, D. H. Liebenberg, and J. C. Bronson, Phys. Rev. B **21**, 5137 (1980).
[33] J. P. Hansen and E. L. Pollock, Phys. Rev. A **5**, 2651 (1972).
[34] M. A. Morales, S. Hamel, K. Caspersen, and E. Schwegler, Phys. Rev. B **87**, 174105 (2013).

[35] X. Jiang, Y. Zheng, X.-X. Xue, J. Dai, and Y. Feng, J. Chem. Phys. **152**, 074701 (2020).

[36] Y. Wang, X. Zhang, S. Jiang, Z. M. Geballe, T. Pakornchote, M. Somayazulu, V. B. Prakapenka, E. Greenberg, and A. F. Goncharov, J. Chem. Phys. **150**, 114504 (2019).

[37] M. W. Wong, J. Amer. Chem. Soc. **122**, 6289 (2000).

[38] R. T. Howie, I. B. Magdău, A. F. Goncharov, G. J. Ackland, and E. Gregoryanz, Phys. Rev. Lett. **113**, 175501 (2014).

[39] I. B. Magdău and G. J. Ackland, Phys. Rev. Lett. **118**, 145701 (2017).

[40] C. S. Yoo (private communication).